International Journal of Fluid Machinery and Systems
Vol. 1, No. 1, October-December 2008

Original Paper

Return Vane Installed in Multistage Centrifugal Pump

Masafumi Miyano[1], Toshiaki Kanemoto[2], Daisuke Kawashima[1], Akihiro Wada[3], Takashi Hara[3] and Kazuyuki Sakoda[3]

[1]Graduate, Graduate School of Engineering, Kyushu Institute of Technology
[2]Faculty of Engineering, Kyushu Institute of Technology
Sensui 1-1, Tobata, Kitakyushu, 804-8550, Japan
[3]Research & Development Department, Torishima Pump Manufacturing Co., Ltd.
Miyata 1-1-8, Takatsuki, 569-8660, Japan

Abstract

To optimize the stationary components in the multistage centrifugal pump, the effects of the return vane profile on the performances of the multistage centrifugal pump were investigated experimentally, taking account of the inlet flow conditions for the next stage impeller. The return vane, whose trailing edge is set at the outer wall position of the annular channel downstream of the vane and which discharges the swirl-less flow, gives better pump performances. By equipping such return vane with the swirl stop set from the trailing edge to the main shaft position, the unstable head characteristics can be also suppressed successfully at the lower discharge. Taking the pump performances and the flow conditions into account, the impeller blade was modified so as to get the shock-free condition where the incidence angle is zero at the inlet.

Keywords: Centrifugal pump, return vane, multistage, performance, impeller, swirl stop, unstable performance

1. Introduction

Multistage centrifugal pumps always play an important role in the construction of the future infrastructures for the sustainable developments. The improvement of the pump performances contributes more or less to cope with the warming global environments, and the pumps with the fruitfully advanced technologies are also under obligation to assist such contributions. To accomplish the obligations, the channel profile from the outlet of the impeller to the inlet of the next stage impeller must be optimized more and more so as to bring the impeller with higher efficiency into full performance.

Diffuser vanes, return vanes and impellers have been investigated respectively, and not only the effects of each profile on the pump performances have been investigated experimentally and numerically but also the profiles have been optimized [1]-[7]. Besides, the rotor-stator interactions have been investigated experimentally and numerically to suppress the acoustic noises and the mechanical vibrations [8]-[11], and the flow conditions in the pump composed of the impeller and the stationary components have also been predicted numerically [12]-[14]. The pump profiles will be optimized by the advanced flow simulations in the near future. To mediate between the present and the future technologies of the multistage pump design, this serial research intends to optimize experimentally the channel profile equipped with the diffuser vane and the return vane, taking the interaction to the next stage impeller into consideration. At the first step, this paper discusses experimentally the relation between the return vane profile and the pump performances, paying attention to the inlet flow conditions of the next stage impeller.

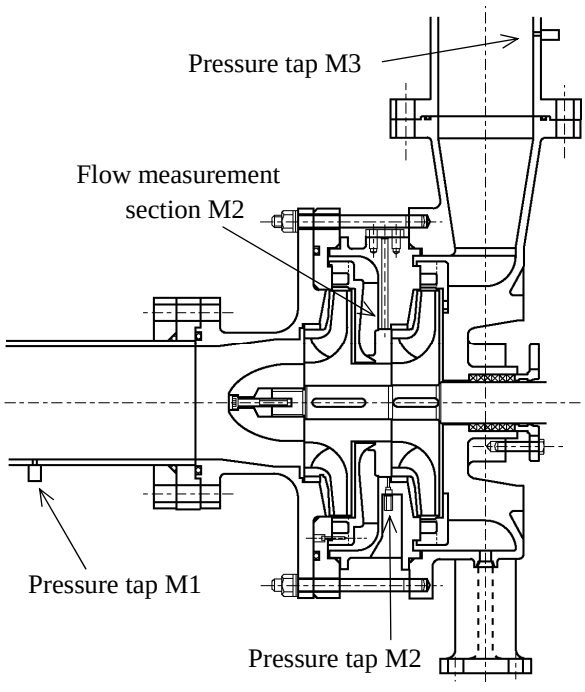

Fig. 1 Model multistage centrifugal pump

Received June 19 2008; revised August 25 2008; accepted for publication August 27 2008: Review conducted by Prof. Tong-Seop Kim.
Corresponding author: Toshiaki Kanemoto, turbo@tobata.isc.kyutech.ac.jp

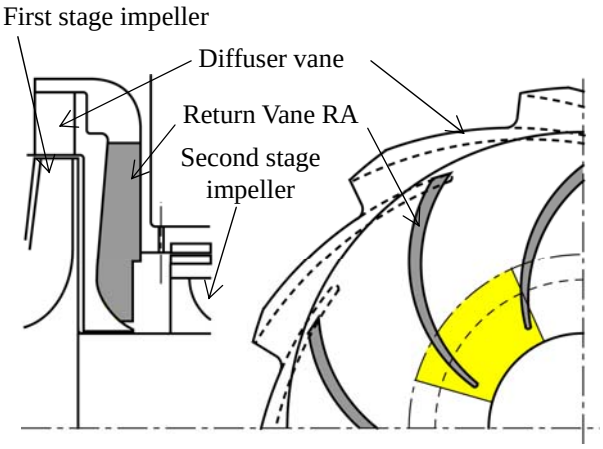

(a) Return Vane RA

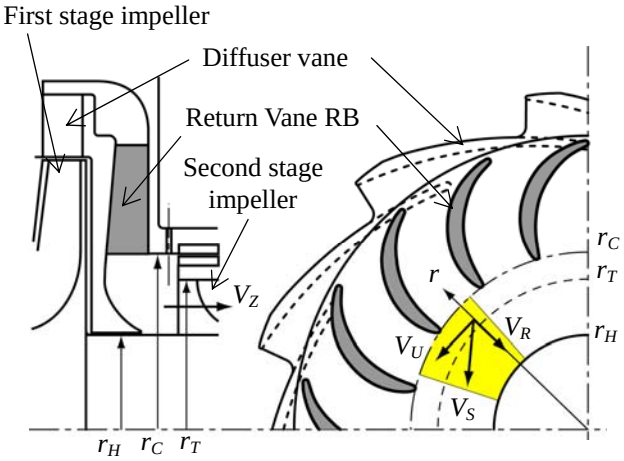

(b) Return Vane RB

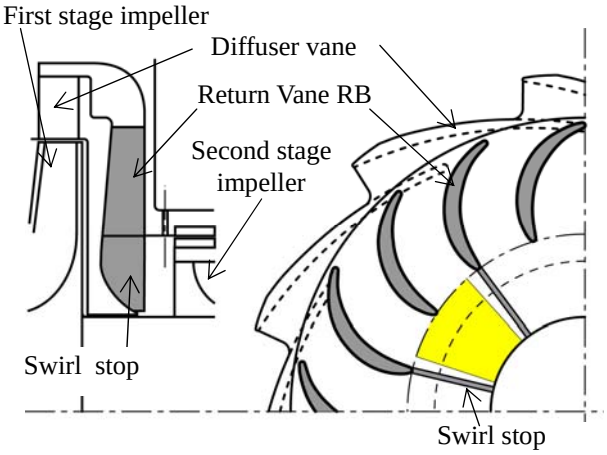

(c) Return Vane RC

Fig. 2 Return vane profiles

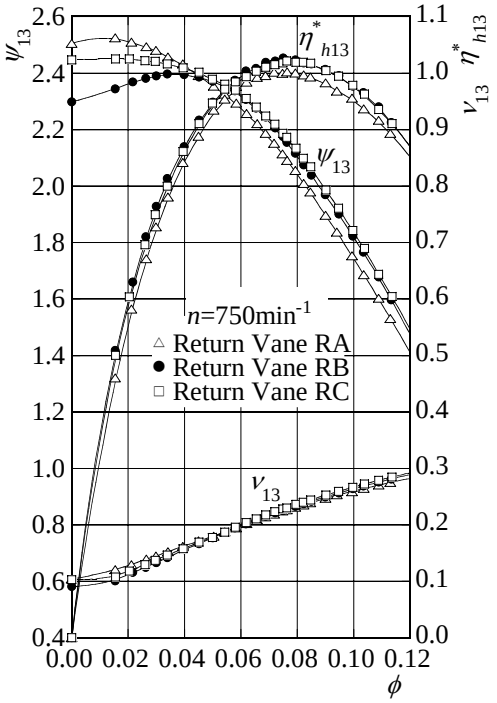

Fig. 3 Performances of the model pump (M1-M3)

Besides, the desirable impeller profile is proposed on the basis of the above discussions. The effect of the diffuser vane profile on the multistage pump performances will be discussed at the next paper, taking account of matching the diffuser vane with the return vane and the next stage impeller.

2. Model Centrifugal Pump

2.1 Profile of Model Pump

Figure 1 shows the model multistage centrifugal pump which is composed of the suction pipe, the first stage impeller, the 11 diffuser vanes, the U-turn channel, the return vane prepared below, the annular channel, the second stage impeller, the diffuser vanes, the discharge chamber, and the discharge pipe. Both impellers have the same profile with 7 blades and are called Impeller A in the prototype, where the suction and the delivery diameters are 170 mm and 300 mm, while the specific speed per the stage is 170 (m, m^3/min, min^{-1}) at the design point with the discharge coefficient ϕ =0.105 [=Q/Au_2, Q: the discharge, A: the impeller outlet area, u_2: the peripheral velocity at the impeller outlet]. The cross sectional area of the discharge chamber just downstream of the second stage diffuser vane is temporarily kept constant in the tangential direction. The length of the annular channel downstream of the return vane, namely upstream of the second stage impeller, may be longer than that of the prototype, to measure experimentally the flow conditions.

2.2 Return Vanes

The return vanes installed in the above model pump are shown in Fig. 2, where these leading edges are set at the same radius. As for Return Vane RA, eleven vanes are installed in the channel. The trailing edge with the vane outlet having an angle 75 degrees measured from the tangential direction is in close to the main shaft, but the latter half of the return vane does not have the end wall and is opened to the downstream annular channel with the inner and the outer radii r_H and r_C. Therefore, the return vane may discharge the swirling flow into the downstream channel, but may serve as the swirl stop. Return Vane RB was designed with the numerical simulation by means of the singularity method in the potential flow field, so as to discharge the swirl-less flow [15], where the datum flow averaged at the return vane inlet was predicted by the commercial code SCRYU/Tetra with the k-ε

turbulent model. The trailing edge is set at the radius r_C corresponding to the outer wall of the downstream annular channel. The vane number is 18 and the vane thickness was determined so as to make the total area of the 18 vane sections coincide with that of the 11 sections of Return Vane RA. Besides, Return Vane RC composed of 18 Return Vanes RB with the 9 swirl stops shown in Fig. 2(c) was also prepared.

3. Pump Performances

3.1 Performances of Model Pump

The performances of the model pump set in the open test loop while operating at the rotational speed of n=750 min^{-1} are shown in Fig. 3, where ψ is the head coefficient [$=H/(u_2^2/2g)$, H: the total head, g: the gravitational acceleration], ν is the shaft power coefficient [$=P/(\rho A u_2^3/2)$, P: the shaft power without the mechanical power loss such as the bearings], η^*_h is the hydraulic efficiency divided by the maximum hydraulic efficiency of the two-stage model pump equipped with Return Vane RA [$=\eta_h/\eta_{hA13max}$, $\eta_h=\rho gQH/P$]. Besides, the subscript 13 means the values as the two-stage model pump, and the head H was estimated with the static pressure and the mean meridian velocity at Sections M1 and M3 (see Fig. 1). The head of the model with Return Vane RA is lower at the higher discharge and is higher at the lower discharge, as compared with that with Return Vane RB or RC. The head of the model with Return Vane RB has the rising portion of the characteristics, where the head increases with the increase of the discharge, in close to the shut off operation, but the swirl stop suppresses successfully such characteristics (see ψ_{13} of the model with Return Vane RC). The head affects mainly the hydraulic efficiency. That is, the maximum efficiency of the model with Return Vanes RB or RC is about 1.5 % higher than that with Return Vane RA, while these efficiencies η^*_{h13} are also higher irrespective of the discharge.

3.2 Stage Performances

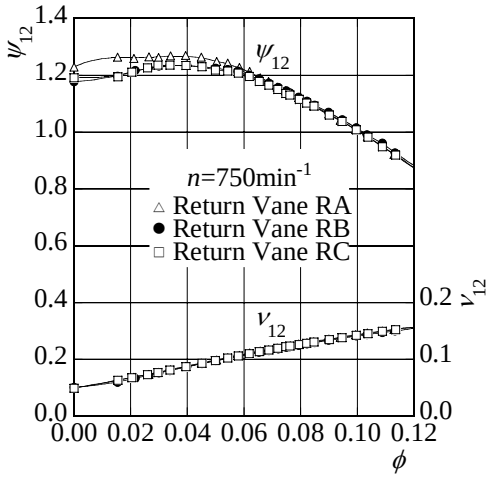

(a) First stage (M1-M2)

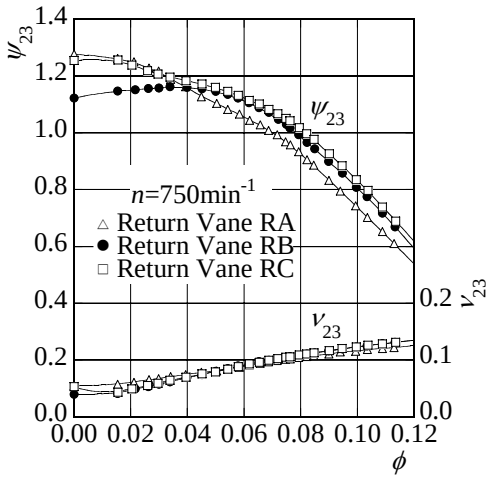

(b) Second stage (M2-M3)

Fig. 4 Pump performances of each stage

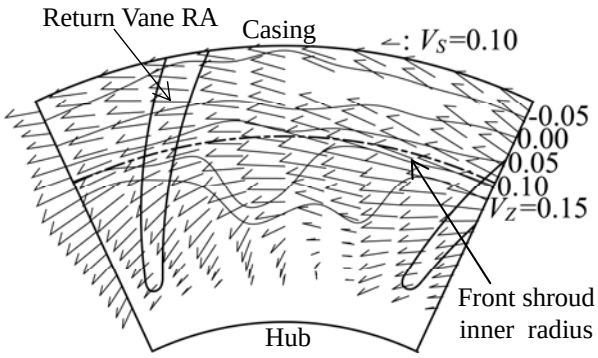

(a) Return Vane RA

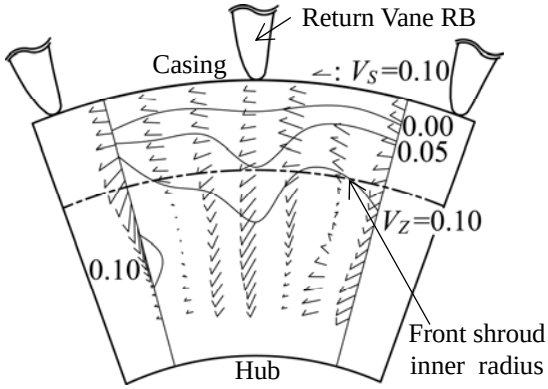

(b) Return Vane RB

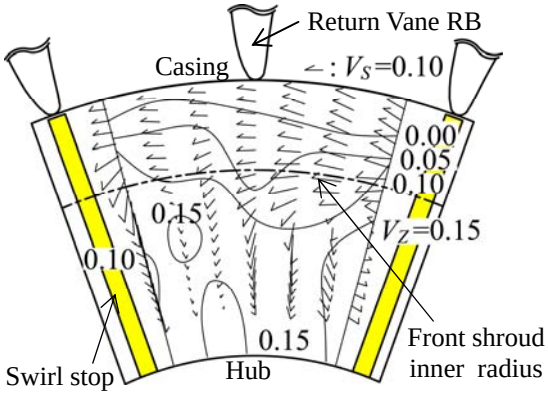

(c) Return Vane RC

Fig. 5 Flow conditions at SectionM2 (ϕ=0.105)

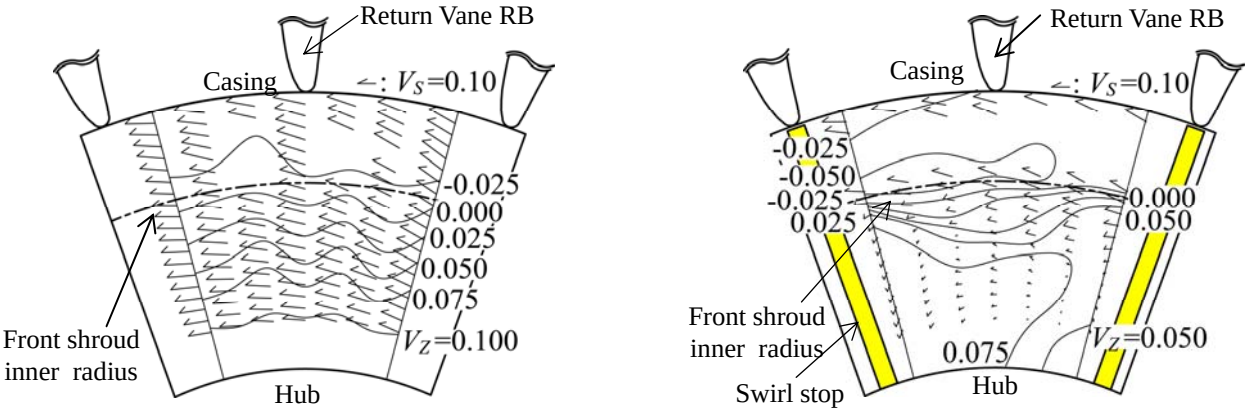

(a) Return Vane RB (b) Return Vane RC

Fig. 6 Effect of the swirl stop on flow conditions at Section M2 (ϕ=0.022)

To discuss the performances in detail, the stage performances were investigated as shown in Fig. 4, where the stage was separated at Section M2 (see Fig. 1), subscripts 12 and 23 stand for the values of the first and the second stages respectively. The shaft power coefficient of the first stage, ν_{12}, was measured by eliminating the front shroud and the blades from the second stage impeller, and the coefficient of the second stage is $\nu_{23}=\nu_{13}-\nu_{12}$. The head at Section M2 was estimated easily from the static pressure at the outer wall and the mean axial velocity though the annular channel has the curvature. The head is 1.5-2.4% lower than the total pressure head measured by the Pitot tube on the cross section at ϕ=0.105. Besides, the cross sectional area of the discharge chamber just downstream of the second stage diffuser vane is kept constant in the tangential direction. These may affect somewhat the quantitative performances of the stage, but the effect of the return vane profile on the performances can be evaluated relatively. The shaft power coefficient ν_{12} of the first stage is scarcely affected by the return vane profile, as recognized in Fig. 4(a). The effect of the return vane profile on the head is also tiny at the higher discharge, and the heads have unstable characteristics in close to the shut off operation because the suction pipe upstream of the first stage impeller does not have the swirl stop.

The effect of the return vane profile on the performances appears obviously in the second stage as shown in Fig. 4(b). The highest head, at the higher discharge, is in the model with Return Vanes RC, then RB, then RA, respectively. At the lower discharge, the head of the model with Return Vane RA is almost the same as that with Return Vane RC, and both heads do not have the rising portion of the characteristics due to the effective work of the swirl stop. On the contrary, the head of the model with Return Vane RB has the rising portion at the lower discharge. Such heads of the second stage control mainly the head of the model pump ψ_{13} shown in Fig. 3.

4. Flow at Return Vane Outlet / Next Stage Impeller Inlet

To match the second stage impeller, namely the next stage impeller in the multistage pump, with the return vane, the flow conditions at Section M2 were measured by the appropriated 5-hole Pitot tube in the steady state conditions, where the measurement region is in one pitch (colored in Fig. 2) of the return vane cascade though the number of the return vane differs from one of the diffuser vane.

4.1 Flow through Cross Section

Figure 5 shows the flow conditions on the cross section while keeping the discharge constant at ϕ=0.105, where the axial velocity component V_Z = (v_z/u_2) is given with the iso-velocity lines, the velocity component parallel to the cross section V_S = (v_s/u_2) is given with the velocity vectors, the return vanes are drawn by the full lines, and the inner radius of the front impeller shroud is denoted by the dotted-and-dashed

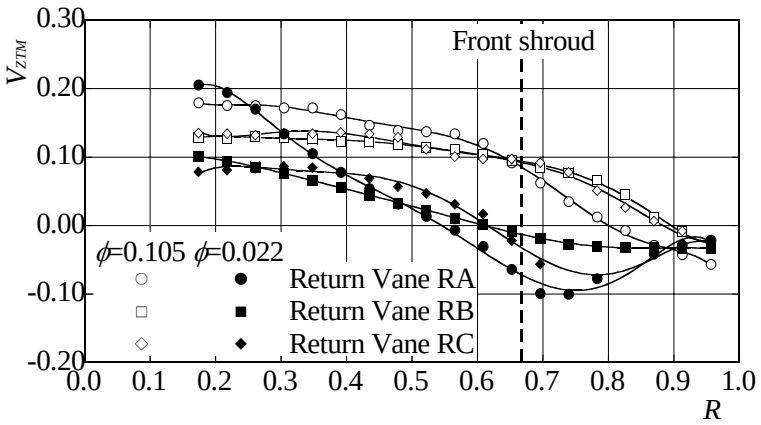

(a) Axial velocity components

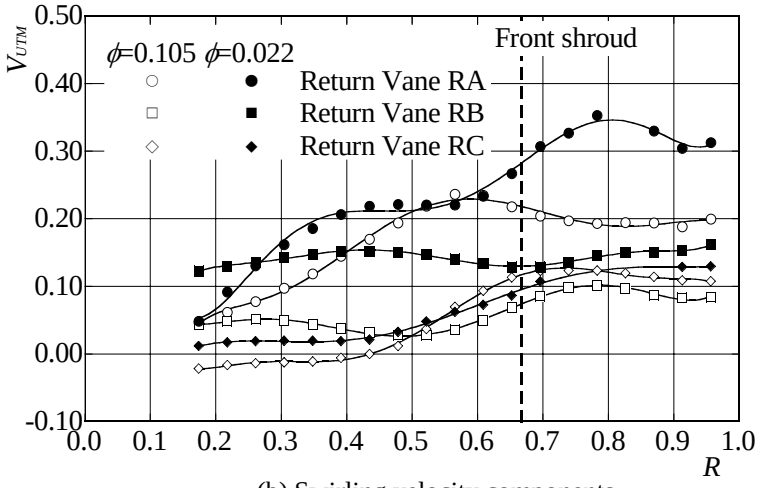

(b) Swirling velocity components

Fig. 7 Mean velocities at Section M2

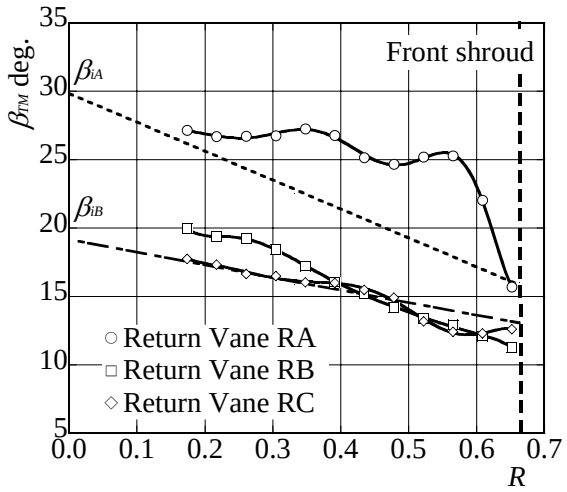

Fig. 8 Relative inlet flow angles for the next stage (ϕ=0.105)

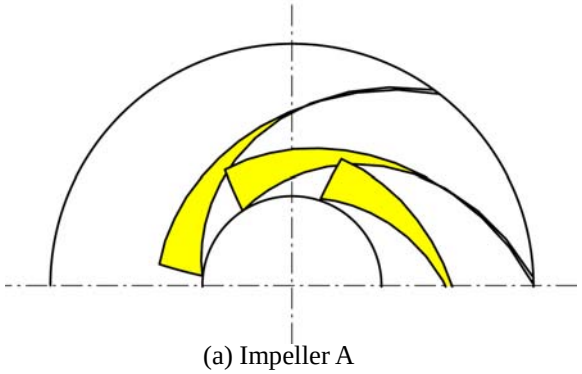

(a) Impeller A

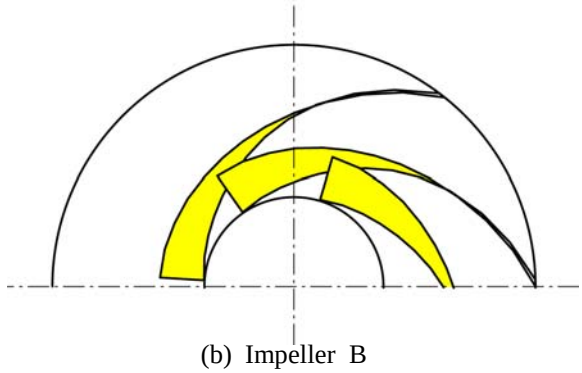

(b) Impeller B

Fig. 9 Impeller profiles

line. Return Vane RA can not remove the swirling velocity component as presumed at the vane design, and the reverse flow appears in close to the casing wall. On the contrary, Return Vane RB can remove successfully the swirling velocity component as expected in the vane design. In such acceptable flow conditions discharging the swirl-less flow, it is not necessary to equip with the swirl stop as the flow condition of the model with Return Vane RC is almost the same as that with Return Vane RB. The swirling velocity component at this section affects directly the impeller work at the next stage, and the head of the model with Return Vane RA, ψ_{23}, is lower than that with the other return vane (at the higher discharge in Fig. 4).

4.2 Effect of Swirl Stop

The flow conditions at the lower discharge, ϕ= 0.022, are shown in Fig. 6. The swirling velocity component is also induced from the impeller rotation in the next stage as well known, and the component is observed obviously in the model with Return Vane RB even at Section M2 [see Fig. 6(a)]. The component, however, is suppressed well by equipping with the swirl stop [Return Vane RC, see Fig. 6(b)], and the swirl-less flow at the impeller inlet increases the impeller work, namely the head. Resultantly, the head in the model with Return Vane RA or RC does not have the rising portion of the characteristics at the lower discharge, as shown before. That is, the swirl stop of Return Vane RC or the latter half of Return Vane RA contributes successfully to suppress the unstable performance.

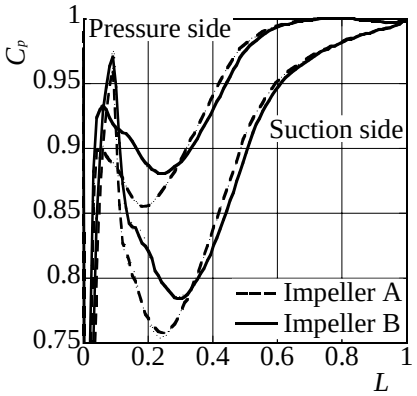

Fig. 10 Pressure distributions on impeller blade surfaces

4.3 Mean Flow Condition

The mean flow averaged in the tangential direction at the same radius of the cross section, Section M2, is shown in Fig. 7, where V_{ZTM} and V_{UTM} (positive in the rotational direction of the impeller) are the axial and swirling velocity components divided by u_2, while R is the dimensionless radius divided by the channel width, and the dashed line gives the inner radius of the front shroud. The swirling velocity components V_{UTM}, which are promoted more or less by the shroud rotation, become faster with the increase of the radius, irrespective of the return vane profile and the operation point, namely the discharge. On the other hand, the axial velocity components V_{ZTM} become slower, and the reverse flow appears in close to the casing wall at the low discharge, as shown before. The flow condition of the model with Return Vane RB is also similar to that with Return Vane RC at the higher discharge. The swirling velocity component of the model with Return Vane RC, however, is scarcely affected by the discharge and is tiny at the radius smaller than R=0.5. On the contrary, the flow conditions of the model with Return Vane RA are remarkably distorted in the radial direction, especially at the low discharge, and such distortion may cause the increase of the mixing loss in the downstream.

Figure 8 shows the relative flow angle β_{TM} measured from the tangential direction, which is obtained from the flow given in Fig. 7 and the peripheral velocity at the impeller inlet, where the dotted line gives the blade inlet angle β_{iA} of Impeller A presented in this paper. Return Vane RA gives the negative incidence angle to the second stage impeller which corresponds to the operation at the higher discharge, but Return Vanes RB and RC give the positive incidence angle which corresponds to the operation at the lower discharge. That is, the second stage has the shock loss at the impeller inlet irrespective of the return vane profile, while ϕ=0.105. To get the shock-free condition where the incidence angle is zero, irrespective of the radius, the blade inlet angle may as well be modified as β_{iB} in Fig. 8 for Return Vane RB or RC, which is estimated in the uniform flow without the swirl at ϕ=0.105. The angle is also acceptable for the first stage impeller, as for getting the shock-free.

5. Modification of Impeller

5.1 Impeller Profile

The impeller with the desirable blade inlet angle β_{iB} given in Fig. 8 was prepared for the model with Return Vane RB or RC, to get the shock-free condition at the normal operation. The impeller profile called Impeller B is shown in Fig. 9, in comparison with Impeller A presented in the previous discussions. The meridian view, the blade number, and the blade thickness are the same as those of Impeller A, but the blade inlet angle is smaller than that of Impeller A. The blade outlet angle of 28 degrees measured from the tangential direction is also the same as that of Impeller A, to get the same theoretical head. The blade camber was determined to get the moderate pressure distribution along the blade surfaces, which were predicted by the singularity method [15], while the cross section of the passage is rectangle as much as possible. The blade length of Impeller B with the smaller blade inlet angle is slightly longer than that of Impeller A. The predicted pressure distributions on the blade surfaces at the hub are shown in Fig. 10, where L is the dimensionless surface length measured from the leading edge and C_P is the pressure coefficient based on the upstream flow. The pressure difference between both impellers appears obviously near the inlet on the pressure surface.

5.2 Pump Performances

The effect of the impeller profile on the pump performances of the model with Return vane RB, which gives the good pump efficiency η^*_{h13} as confirmed in Fig. 3, is shown in Fig. 11. Impeller B makes the head ψ_{13} and the hydraulic efficiency η^*_{h13} somewhat higher. It may not be expected, however, to improve the performances at the higher discharge because the blade inlet angle of Impeller B is suitable for the lower discharge as compared with Impeller A.

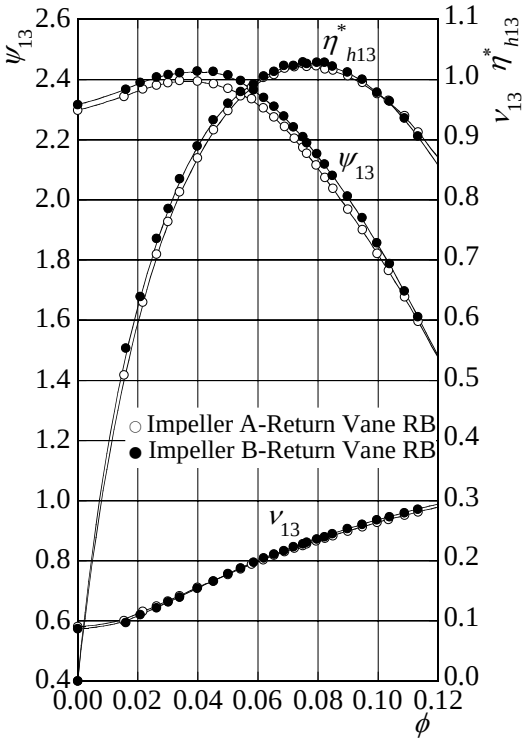

Fig. 11 Effect of impeller profile on model pump performances (M1-M3)

6. Concluding Remarks

The effects of the return vane profile on the pump performances and the flow conditions downstream of the return vane, namely upstream of the next stage impeller were investigated experimentally. The return vane, whose trailing edge is set at the outer wall radius of the downstream annular channel and which discharges the swirl-less flow, gives the well pump performances. By equipping such return vane with the swirl stop from the trailing edge to the main shaft, he unstable head characteristics can be suppressed successfully at the lower discharge. Taking the discussions about the pump performances and the flow conditions into account, the impeller blade was modified so as to get the shock-free condition at the inlet. The blade length of the modified impeller (Impeller B) with the smaller blade inlet angle is slightly longer than that of the usual Impeller (Impeller A), and the modified impeller improves slightly the pump efficiency.

Acknowledgments

The authors wish to thank to the 22th (2002) Harada Memorial Foundation in Japan, which co-sponsors some parts of this research.

Nomenclature

A	impeller outlet area
C_P	pressure coefficient based on the flow at the upstream of the impeller
H	total head of the pump
P	shaft power without the mechanical power loss such as the bearings
Q	discharge
R	radius divided by the channel width
V_Z	axial velocity component, divided by u_2
V_S	velocity component parallel to the cross section, divided by u_2
V_{ZTM}	mean axial velocity component averaged in the tangential direction at the same radius of the cross section, divided by u_2
V_{UTM}	mean swirling velocity component averaged in the tangential direction at the same radius of the cross section, divided by u_2
g	gravitational acceleration
n	rotational speed of the impeller
u_2	peripheral velocity at the impeller outlet

β_{TM} relative flow angle measured from the tangential direction
β_{iA}, β_{iB} blade inlet angles of Impellers A and B
η^*_h hydraulic efficiency divided by the maximum hydraulic efficiency of the two-stage model pump equipped with Return Vane RA [$=\eta_h/\eta_{hA13max}$, $\eta_h=\rho gQH/P$].
ν shaft power coefficient [$=P/(\rho A u_2^3/2)$]
ρ water density
ϕ discharge coefficient [$=Q/Au_2$]
ψ head coefficient [$=H/(u_2^2/2g)$]

subscripts 13, 12, 23 values of the two-stage, the first stage and the second stage

Impellers A, B see Fig. 9
Return Vanes RA, RB, RC see Fig. 2

References

[1] Li, J., Okamura, T., and Tsukamoto, H., 2004, "Optimization of Low Solidity Diffuser for Diffuser Pump by Genetic Algorithm", Proceedings of the 22nd IAHR Symposium, CO-ROM B12-1.doc1-12(12).
[2] Saito, S. and Sakurai, T, 2000, "Effects of Diffuser Profile on Hydraulic Performance of Low Specific-Speed Mixed Flow Pump", Turbomachinery, Vol. 28, No.10, pp. 598-607, in Japanese.
[3] Sakutai, T., Kaneko, A., Enomoto, T. and Hagino, M., 2007, "Development of Centrifugal Pump with Adjustable Guide Vane", Proceedings of the 9th Asian International Conference on Fluid Machinery, CD-ROM:AICFM9-059.
[4] Hara, T., Fukuda, T. and Wada A., 2002, "The study of Hydraulic Characteristic of Multi-stage Pumps", Torishima Review, No. 16, pp. 32-37, Torishima Pump, in Japanese.
[5] Schilling, R. et al., 1983, "Investigation of the Fluid Flow within the Return Passage of Multi-Stage Centrifugal Pumps, Proc. 7th Conf. Fluid Machinery, Budapest, pp. 761-769, Akadeniai Kaido.
[6] Kanemoto, T., Yamada, H. and Suzuki, T., 2001, "Effects of Return Vane Outlet Profile in the Meridian Section on Flow at the Next-Stage Impeller", Turbomachinery, Vol. 29, No. 10, pp.626-631, in Japanese.
[7] Kassai, N., Miyauchi, S. and Fukutomi, J., 2007, "Optimization Design of Pump Impeller", Proceedings of the 9th Asian International Conference on Fluid Machinery, CD-ROM:AICFM9-041.
[8] Tsugawa, T, 2007, "The Relation between Solidity and the Other Shape Factors for Complete Optimum Meridian Profile of Impeller with Guide Vane", Proceedings of the 5th Joint ASME/JSME Fluid Engineering Conference, CD-ROM:FEDSM2007-37344.
[9] Sano, T., Kobayashi, K., Miyagawa, K., Yamamoto, Y. and Mitsui N., 2007, "Development of High Performance Multistage Centrifugal Pump", Proceedings of the 9th Asian International Conference on Fluid Machinery, CD-ROM:AICFM9-282.
[10] Sugimura, K., Obayashi S. and Jeong, S., 2007, "Multi-objective Design Exploration of a Centrifugal Impeller Accompanied with a Vaned Diffuse", Proceedings of the 5th Joint ASME/JSME Fluid Engineering Conference, CD-ROM:FEDSM2007-37502.
[11] Pavesi., G., Cavazzini, G., Dupont, P., Coudert, S., Caignaert, G., Bois, G. and Ardizzon, G., 2006, "Analysis of Rotor-Stator Interactions Effects within the Vaned Diffuser of a Radial Flow Pump", Proceedings of the 23rd IAHR Symposium, CD-ROM:F206.pdf.
[12] Yamanishi, N., Kato, C., Okita, K. and Motomura T., 2007, "Large Eddy Simulation of Unsteady Flow in the LE-7A Liquid Hydrogen Pump", Proceedings of the 43th AIAA/ASME/SAE/ASEE Joint Propulsion Conference & Exhibit, AIAA 2007-5515.
[13] Huang, S., 2006, "A Numerical Study on the Impeller-diffuser Interactions of a Multi-stage Centrifugal Pump", Proceedings of the 23rd IAHR Symposium, CD-ROM:F172.pdf.
[14] Berten, S., Farhat, M., Dupont P. and Avellan F., 2007, "Rotor-Stotor Interaction Induced Pressure Fluctuations: CFD and Hydroacoustic Simulations in the Stationary Components on a Multistage Centrifugal Pump", Proceedings of the 5th Joint ASME/JSME Fluid Engineering Conference, CD-ROM:FEDSM2007-37549.
[15] Toyokura, T., Kanemoto, T. and Hatta, M., 1986, "Study on Circular Cascades for Return Channel of Centrifugal Turbomachinery (1st Report: Inverse Method and Cascade Design)", Bulletin of the JSME, Vo.l. 52, No. 473, pp.50-58.